Ioannis Vayas
Aristotelis Charalampakis
Vlasis Koumousis

DOI: 10.1002/stco.200910018

Inelastic resistance of angle sections subjected to biaxial bending and normal forces

Steel trusses and other structures with angle section members are usually designed by elastic methods. This may lead to uneconomical designs when these sections are subjected – besides the axial force – to biaxial bending arising not only from eccentric connections, but also from direct transverse loading. This paper provides a simple inelastic interaction formula, Eq. (14), as well as an enhanced inelastic formula, Eq. (27), for the combination of axial force and bending moments about the principal axes which may be used for angle cross-sections of classes 1 or 2. The formulae do not always exhaust the full plastic cross-sectional resistance but do lead to a more economical design of the section, especially when bending is dominant. The formulae cover only the design of the cross-section and do not address stability considerations.

1 Introduction

Angle sections are widely used as truss members due to their easy connections to adjacent members. Typical examples are lattice towers for telecommunications purposes, where equal leg angles are often used for tower legs and bracing members (Fig. 1). Truss members are primarily subjected to axial forces. Bending moments arise mostly from eccentricities at the connections because angles are connected by one or more bolts in one leg. However, in telecommunications towers, angle sections are also subjected to bending due to direct transverse wind loading and the fact that the legs are continuous over the full height, meaning that they have to be designed for biaxial bending and normal forces. For such towers, the axial force dominates in the lower part due to high overturning moments, whereas bending may dominate in the upper part due to the higher wind forces.

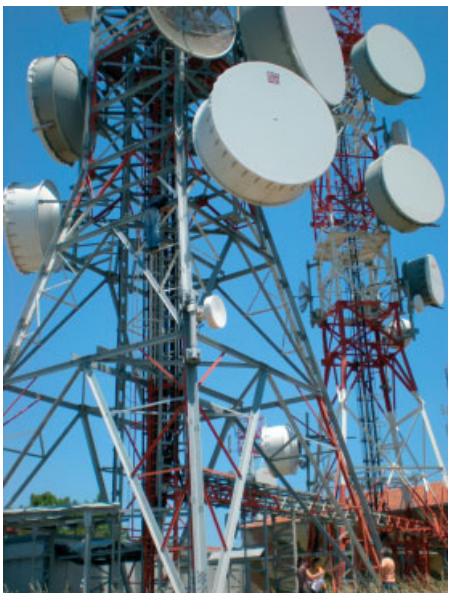

Fig. 1. Examples of telecommunications towers with angle sections

Angle sections are usually designed by elastic methods, where stresses are determined separately for the (factored) design moments and forces, and the resulting stresses are limited by the design strength, this being the yield stress divided by the partial factor for resistance γ_{M0}. However, the application of the theory of elasticity for the verification of angles leads to uneconomic designs due to their small elastic moment capacity, especially for bending about the weak axis and the linear superposition of stresses arising from bending moments and normal forces.

Modern codes of practice like Eurocode 3 [1] allow for the use of inelastic design methods for compact cross-sections of classes 1 or 2, where the bending resistance is not reduced due to local buckling. These codes provide plastic interaction formulae for biaxial bending and normal forces for doubly symmetrical I, H and box sections. Improved interaction formulae for the same types of cross-section, including the effects of warping torsion, were proposed by *Vayas* [2], [3]. *Scheer* and *Bahr* [4] provided inelastic interaction diagrams for angle sections subjected to eccentric axial forces. However, codes of practice do not generally cover inelastic design of angle sections. In an effort to overcome this deficit, the present paper treats the inelastic design of equal leg angle cross-sections subjected to biaxial bending and axial force. It covers fully the design of the angle if the design actions arise from second-order theory, possibly including imperfections. Otherwise, a stability check of the member design is required in addition.

2 Notation

The dimensions and axes of the cross-section from [1] are given in Fig. 2a.

A	cross-sectional area
N	normal force
M_u, M_v	bending moments, major and minor principal axes

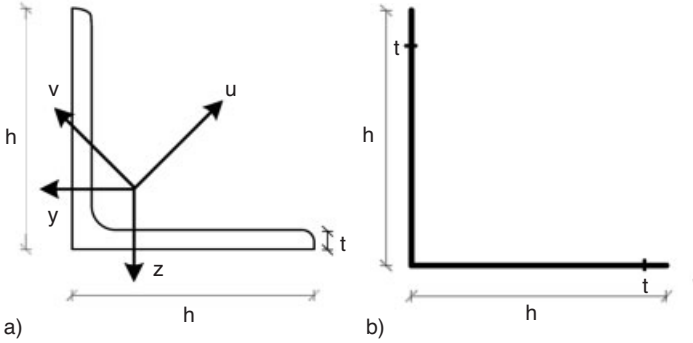

Fig. 2. Angle section: a) dimensions and axes, and b) idealization

N_{pl}	plastic resistance to normal force
$W_{u,pl}$, $W_{v,pl}$	plastic section moduli, major and minor principal axes
$M_{u,pl}$, $M_{v,pl}$	plastic bending moments, major and minor principal axes
f_y	yield strength
$n = N/N_{pl}$	ratio of normal force to plastic resistance to normal force
$m_u = M_u/M_{u,pl}$	ratio of bending moment to plastic bending moment, major principal axis
$m_v = M_v/M_{v,pl}$	ratio of bending moment to plastic bending moment, minor principal axis

3 Plastic forces and moments

Under the assumption that the leg thickness t is small compared with the leg length h, the cross-section may be idealized as shown in Fig. 2b. Alternatively, the cross-section could be idealized by the centre-lines of the legs, meaning that the relevant lengths would be $h' = h - t/2$. In such a case all relations given below are still valid when h is substituted by h′. For angles with h = 10t, the cross-sectional area of the adopted model given in Eq. (4) is 4–5 % higher, whereas for the alternative model it is 5–6 % less than the true area. However, this error can be eliminated if the cross-sectional area A is not calculated for the idealized model but instead is taken from the relevant section tables. Concerning the material behaviour, a bi-linear elastic-plastic material law is assumed.

The stress distributions due to axial forces and bending moments acting alone are given in Fig. 3, and the stress resultants for each leg in Fig. 4. Tension is positive. The figures show that the plastic neutral axes for both strong and weak axis bending coincide with the principal elastic axes u-u and v-v. It should be noted that whereas this holds true for the idealized section shown in Fig. 2b, this is not the case for the true angle section shown in Fig. 2a, for which the plastic neutral axis v-v shifts towards the corner.

The plastic resistances are as follows:

Normal force: $$N_{pl} = A \cdot f_y \tag{1}$$

Bending about the major axis: $$M_{u,pl} = W_{u,pl} \cdot f_y \tag{2}$$

Bending about the minor axis: $$M_{v,pl} = W_{v,pl} \cdot f_y \tag{3}$$

For the idealized section, the cross-sectional area and the plastic section moduli are determined as follows:

$$A = 2 \cdot h \cdot t \tag{4}$$

$$W_{u,pl} = 2 \cdot \frac{A}{2} \cdot \frac{h}{2 \cdot \sqrt{2}} = \frac{A \cdot h}{2 \cdot \sqrt{2}} \tag{5}$$

$$W_{v,pl} = 2 \cdot \frac{h^2 \cdot t}{4 \cdot \sqrt{2}} = \frac{A \cdot h}{4 \cdot \sqrt{2}} \tag{6}$$

Accordingly,

$$M_{u,pl} = \frac{N_{pl} \cdot h}{2 \cdot \sqrt{2}} \tag{7}$$

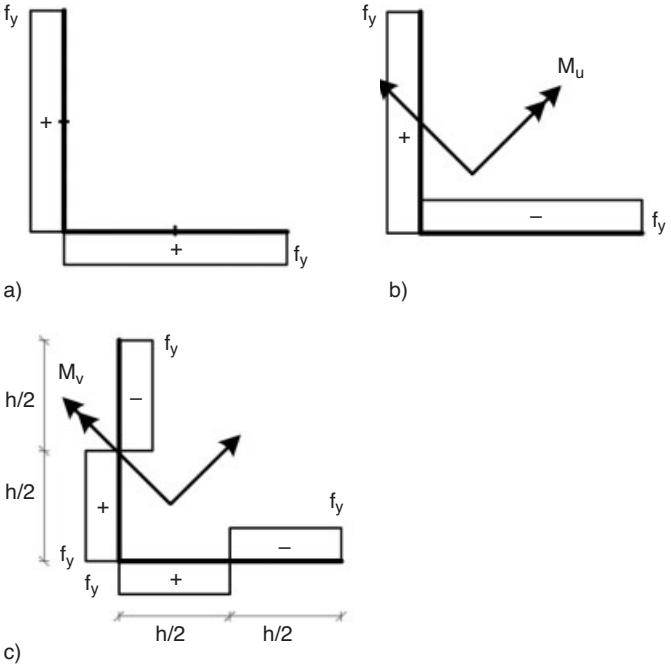

Fig. 3. Stresses due to N, M_u and M_v

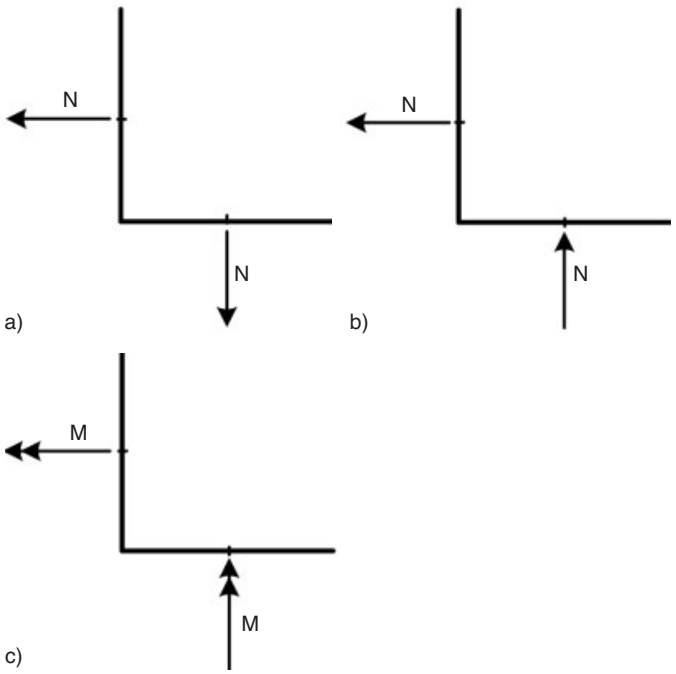

Fig. 4. Stress resultants in legs due to N, M_u and M_v

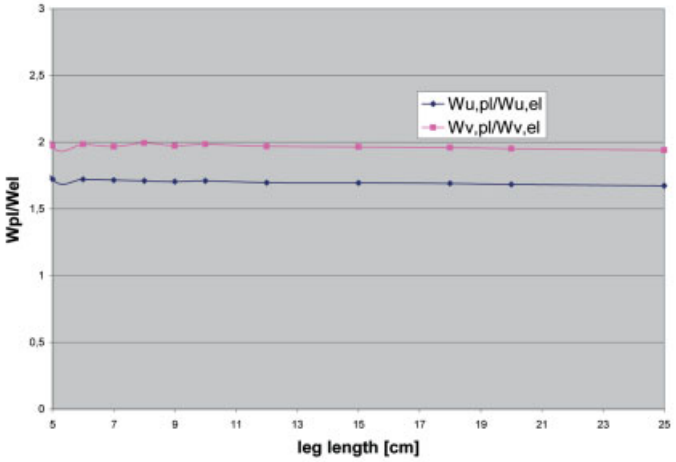

Fig. 5. Ratio of plastic to elastic section moduli for angles with h/t = 10

$$M_{v,pl} = \frac{N_{pl} \cdot h}{4 \cdot \sqrt{2}} = \frac{M_{u,pl}}{2} \tag{8}$$

Fig. 5 shows that for angles with h/t = 10, the W_{pl}/W_{el} ratios are approx. 1.7 for strong axis bending and approx. 2.0 for weak axis bending, and indicate the gain potential in the plastic design of angles.

4 Combination N + M_v

The stress distribution and the stress resultants in each leg for combined axial force and bending about the weak axis are given in Fig. 6. The axial force is resisted by stresses of equal sign about the leg's middle axis over a width equal to n · h, and the bending moment by stresses of opposite sign in the remaining area.

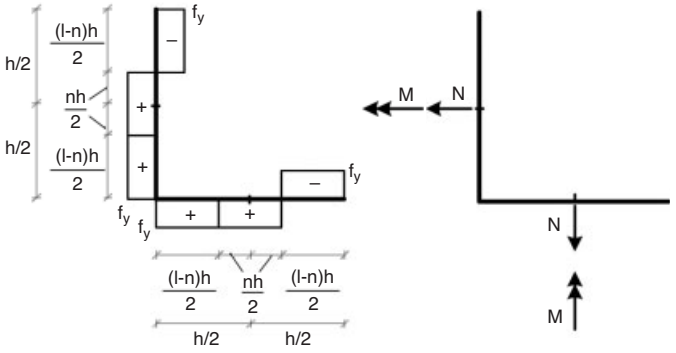

Fig. 6. Stresses and stress resultants in legs due to N + M_v

This stress distribution results in the following minor axis moment, where evidently the stresses about the middle axes of the legs do not make any contribution:

$$M_v = 4 \cdot \frac{1-n}{2} \cdot h \cdot t \cdot f_y \cdot \frac{1+n}{4 \cdot \sqrt{2}} \cdot h = \left(1 - n^2\right) \cdot \frac{N_{pl} \cdot h}{4 \cdot \sqrt{2}} \tag{9}$$

Eqs. (8) and (9) finally yield the plastic interaction relationship, which may be written as:

$$n^2 + m_v = 1 \tag{10}$$

The relevant interaction diagram is plotted in Fig. 7.

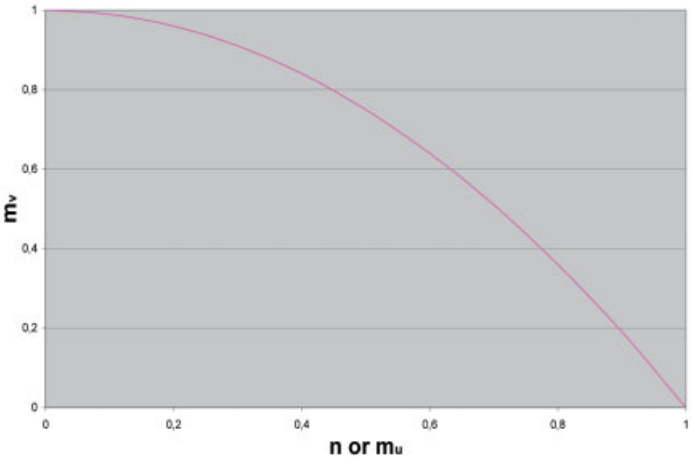

Fig. 7. Inelastic interaction diagram for N + M_v and M_u + M_v

5 Combination M_u + M_v

The stress distribution and the stress resultants in each leg for combined moments about both the strong and weak axes are given in Fig. 8. The moment M_u is resisted by stresses of equal sign, but different in each leg, about the leg middle axis over a width equal to $m_u \cdot h$, and the moment M_v by stresses of opposite sign in the remaining area.

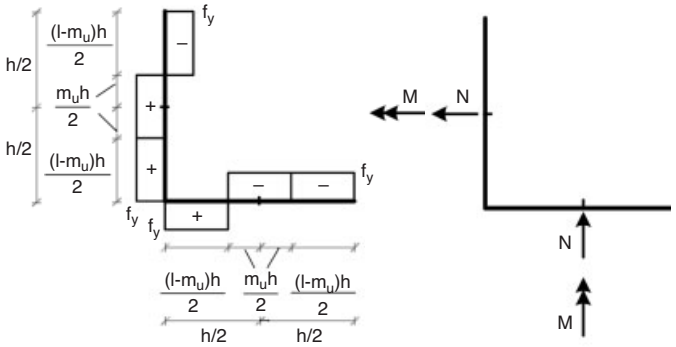

Fig. 8. Stresses and stress resultants in legs due to M_u + M_v

This stress distribution results in the following major axis moment, where evidently only the stresses about the middle axes of the legs make a contribution because the remaining stresses are symmetrical about this axis:

$$M_u = 2 \cdot h \cdot t \cdot f_y \cdot \frac{m_u}{2 \cdot \sqrt{2}} \cdot h = m_u \cdot \frac{N_{pl} \cdot h}{2 \cdot \sqrt{2}} \tag{11}$$

Eqs. (7) and (11) confirm the assumed stress distribution concerning the strong axis bending. Furthermore, the stress distribution assumed results in the following minor axis moment, where evidently the stresses about the middle axes of the legs do not make any contribution because they are symmetrical about the minor bending plastic neutral axis:

$$M_v = 4 \cdot \frac{1-m_u}{2} \cdot h \cdot t \cdot f_y \cdot \frac{1+m_u}{4 \cdot \sqrt{2}} \cdot h = \left(1 - m_u^2\right) \cdot \frac{N_{pl} \cdot h}{4 \cdot \sqrt{2}} \tag{12}$$

Eqs. (8) and (12) finally yield the plastic interaction relationship, which may be written as:

$$m^2_u + m_v = 1 \quad (13)$$

This interaction relationship is similar to Eq. (10) and generates the same interaction diagram as in Fig. 7.

6 Proposed simple formula

Combining Eqs. (10) and (13), the following simple interaction formula is proposed:

$$(|n| + |m_u|)^2 + |m_v| = 1 \quad (14)$$

Eq. (14) is symmetric about both the m_u- and m_v-axes. It is also symmetric with respect to n, i. e. with respect to the m_u-m_v plane in the normalized three-dimensional m_u-m_v-n space. Fig. 9 shows the upper right quadrant of the interaction curve for various values of n.

Fig. 10 shows interaction diagrams for the elastic and plastic design of angles. The elastic curve for n = 0 intersects the two axes at values less than 1 because the elastic moments are smaller than the plastic ones (Fig. 5). It can be seen that the gains offered by plastic design are due, firstly, to the larger plastic moments compared with the elastic ones and, secondly, to the curved form of the interaction diagrams. However, it should be noted that in elastic design the stresses caused by individual forces and moments are added algebraically. That means the elastic interaction diagrams in Fig. 10 correspond to the signs of the forces and moments acting, i. e. negative N (compression), positive M_u, M_v, such that they add up in the extreme fibres. If this is not the case, the elastic diagrams may be much higher.

For the loading case of N + M_u, a simple formulation in the manner of paragraphs 4 and 5 is not straightforward because the asymmetry of the section means that the orientation of the neutral axis is not known. However, as will be demonstrated in the next section, the proposed simple interaction formula, Eq. (14), holds true in an approximate but conservative manner for the generic loading case of N + M_u + M_v.

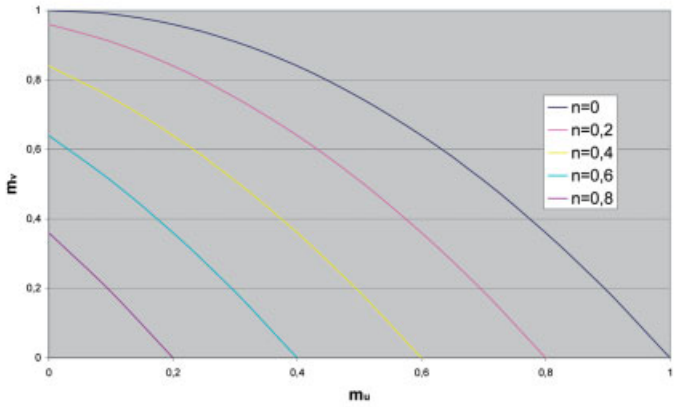

Fig. 9. Inelastic interaction diagram based on the simple interaction formula

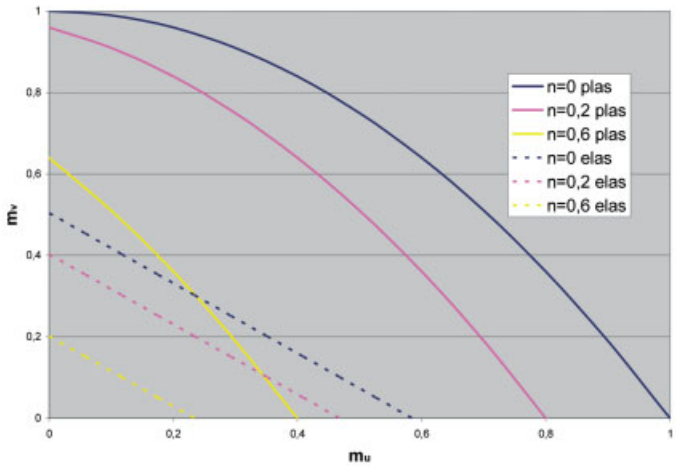

Fig. 10. Interaction diagrams for elastic (under certain conditions) and inelastic design of angles

7 Validation of simple formula

A new generic fibre model algorithm [5] was employed for validation purposes. The algorithm can be used for the analysis of arbitrary sections under biaxial bending and axial load. The geometry of the cross-section is described by curvilinear polygons, i. e. closed polygons with edges that are straight lines or circular arcs. Thus, the angle sections are described exactly by seven-node curvilinear polygons which take into account the curves of the actual section. The stress-strain diagrams of materials consist of any number and any combination of consecutive polynomials. Analytical expressions are utilized for the integration of the stress field even when curved edges are involved.

Fig. 11 shows the results obtained using the code myBiaxial [5] in conjunction with CAD software for the case of the 40 × 40 × 4 mm angle section, n = 0.0 and neutral axis orientation = 50°. The compression zone is shown in red, the tension zone in blue.

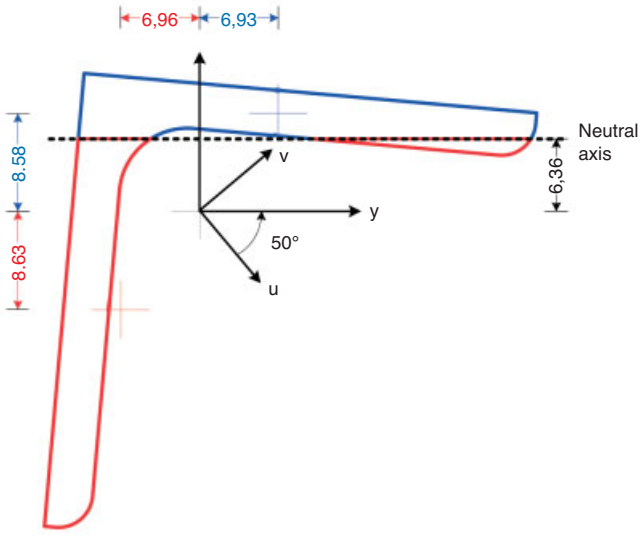

Fig. 11. An instance of a 40 × 40 × 4 mm interaction for n = 0.0 (dimensions in mm)

Neutral axis z-coordinate	6.36 mm
Compression zone (red)	
Centroid, y-coordinate	–6.96 mm
Centroid, z-coordinate	–8.63 mm
Force	–36.09 kN
Tension zone (blue)	
Centroid, y-coordinate	6.93 mm
Centroid, z-coordinate	8.58 mm
Force	36.09 kN

Thus

M_y	0.623 kNm
M_z	–0.502 kNm

Results in global (u,v) reference system

M_u	0.785 kNm
M_v	0.154 kNm

Normalized results

m_u	0.835
m_v	0.316

Using the code myBiaxial, the interaction curves were obtained for n = –0.6, –0.2, 0.0, +0.2 and +0.6 (Fig. 12).

It can be seen that the symmetry with respect to the horizontal axis, i.e. the sign of Mv, is not maintained in the presence of the axial load. The specific case analysed previously (Fig. 11) using CAD software is shown in the same graph by way of a red square.

Next, the interaction curves of Fig. 12 are normalized using the maximum evaluated values of M_u = 0.939 kNm and M_v = 0.487 kNm. Fig. 13 shows the exact interaction curves in solid blue lines, whereas the interaction curves produced by the proposed simple interaction formula are shown as dotted red lines.

The simple interaction formula is based on equilibrium formulae for the cases of N + M_v and M_u + M_v. Thus, a very good approximation is observed for the respective loading cases, as shown by the green dotted points in Fig. 13 and the entire interaction curve that corresponds to n = 0.

The proposed simple interaction formula is conservative for the generic case of N + M_u + M_v, but allows the steel designer to tap safely into the plastic reserves of the section. A more accurate interaction formula that also takes into account the non-symmetry about the horizontal axis of the interaction diagram is proposed in the next section.

8 Enhanced formula

Due to the geometry of the section, the exact position of the neutral axis is not known for the loading case of N + M_u. Moreover, if the direction of the neutral axis is forced to be parallel to the major axis, then satisfying equilibrium yields bending moments about the minor as well as the major axis. Following this path, we obtain information about the corner points of the interaction curves that are marked with red squares in Fig. 13.

The stress distribution of Fig. 14 is valid for n < 0 and results in the following major axis moment:

$$\frac{M_u}{t \cdot f_y} = \frac{h^2}{2 \cdot \sqrt{2}} - \frac{a^2}{2 \cdot \sqrt{2}} + b\frac{h - b/2}{2 \cdot \sqrt{2}} \qquad (15)$$

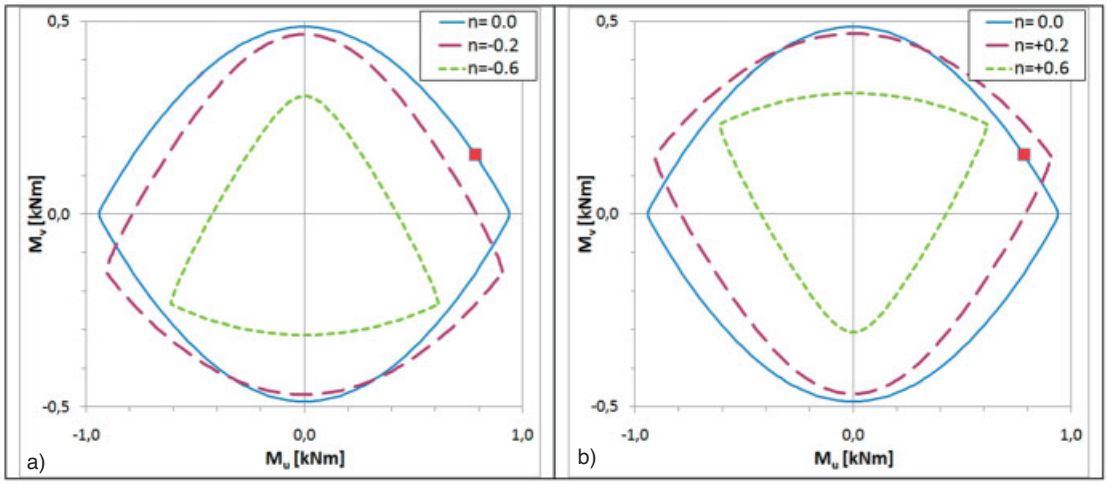

Fig. 12. Interaction curves for a 40 × 40 × 4 mm section subjected to (a) compressive and (b) tensile axial load

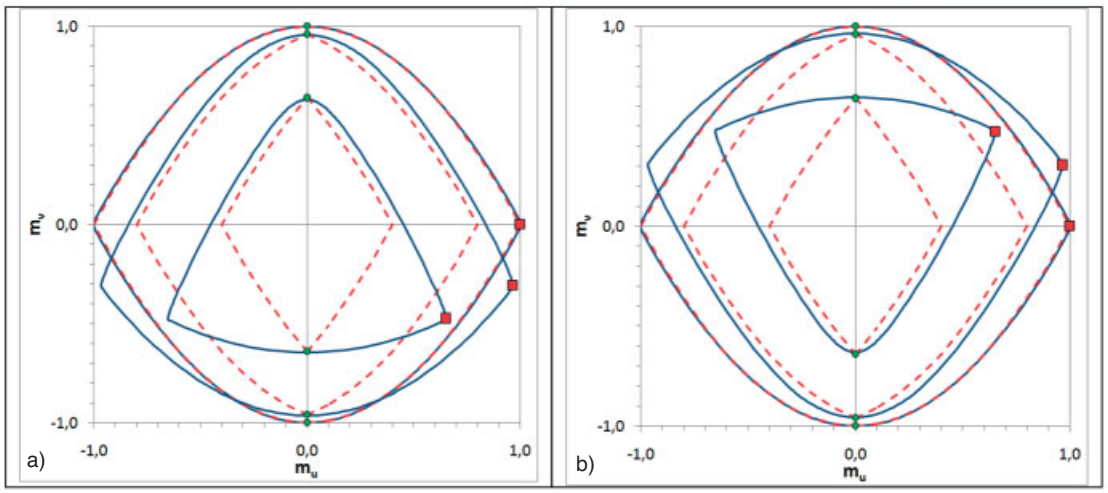

Fig. 13. Interaction curves: exact (blue) and with simple formula Eq. (14) (red dotted) for (a) compression (n = 0, –0.2, –0.6) and (b) tension (n = 0, +0.2, +0.6)

After some algebraic manipulation, Eq. (15) yields:

$$m_u = 1 - n^2,\ n \le 0 \tag{16}$$

Similarly, the stress distribution of Fig. 14 results in the following minor axis moment:

$$\frac{M_v}{t \cdot f_y} = -a\frac{h-a}{2\cdot\sqrt{2}} - b\frac{h-b}{2\cdot\sqrt{2}} \tag{17}$$

After some algebraic manipulation, Eq. (17) yields:

$$m_v = 2n^2 + 2n,\ n \le 0 \tag{18}$$

Eqs. (16) and (18) provide the coordinates (m_u, m_v) of the corner points of the interaction curves that are marked with red squares in Fig. 13a. In particular, the coordinates for n = 0.0, –0.2, –0.6 are evaluated as (0,1), (0.96, –0.32), (0.64, –0.48) respectively.

Seeking to include the aforementioned points in the interaction curve while maintaining its parabolic form, the following expression is employed for the upper part of the interaction curve:

$$(n + \rho_{n1} \cdot |m_u|)^2 + m_v = 1,\ n \le 0,\ 1 - n^2 \ge m_v \ge 2n^2 + 2n \tag{19}$$

where parameter ρ_{n1} is calculated from:

$$\rho_{n1} = \frac{n^2 - n - \sqrt{1 - 4n + 3n^2 + 2n^3 - 2n^4}}{1 - n - n^2 + n^3} \tag{20}$$

Similarly, the following expression is obtained for the lower part of the interaction curve:

$$-(n + \rho_{n2} \cdot |m_u|)^2 + m_v = -1,\ n \le 0,\ n^2 - 1 \le m_v \le 2n^2 + 2n \tag{21}$$

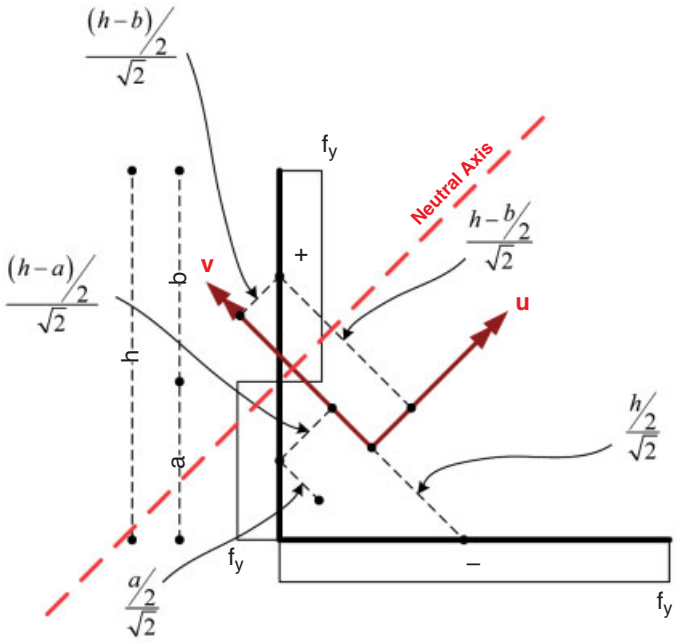

Fig. 14. Stresses for neutral axis orientation parallel to the strong axis with n < 0

where parameter ρ^2 is calculated from:

$$\rho_{n2} = \frac{n^2 - n - \sqrt{1 - n^2 - 2n^3 + 2n^4}}{1 - n - n^2 + n^3} \tag{22}$$

Following similar formulation for the case of a tensile axial load, i.e. n > 0, the upper part of the interaction curve is given as:

$$(n + \rho_{p1} \cdot |m_u|)^2 + m_v = 1,\ n \ge 0,\ 1 - n^2 \ge m_v \ge -2n^2 + 2n \tag{23}$$

where parameter ρ_{p1} is calculated from:

$$\rho_{p1} = \frac{n^2 + n - \sqrt{1 - n^2 + 2n^3 + 2n^4}}{-1 - n + n^2 + n^3} \tag{24}$$

Similarly, for the lower part of the interaction curve:

$$-(n + \rho_{p2} \cdot |m_u|)^2 + m_v = -1,\ n \ge 0,\ n^2 - 1 \le m_v \le -2n^2 + 2n \tag{25}$$

where parameter ρ_{p2} is calculated from:

$$\rho_{p2} = \frac{n^2 + n - \sqrt{1 + 4n + 3n^2 - 2n^3 - 2n^4}}{-1 - n + n^2 + n^3} \tag{26}$$

It can be seen that for n = 0, all ρ parameters are equal to unity and the enhanced formulae are reduced to the simple interaction formula, given by Eq. (14).

Unifying and simplifying Eqs. (19) to (26) for compressive or tensile axial loads as well as for the upper or lower part of the interaction diagram, the enhanced interaction formula may be derived as:

$$\begin{aligned} &\left(|n| + \rho \cdot |m_u|\right)^2 + \rho_s \cdot m_v = 1 \\ &\rho_s = \operatorname{sgn}\left(m_v - 2 \cdot n \cdot \left(1 - |n|\right)\right) \\ &\rho = \left| \frac{n - \operatorname{sgn}(n)\sqrt{1 - 2 \cdot n \cdot \left(1 - |n|\right)\rho_s}}{n^2 - 1} \right| \end{aligned} \tag{27}$$

where sgn(·) is the signum function and sgn(0) = 1. According to Eq. (27), ρ_s = 1 for the upper part of the interaction curve ($m_v \ge 2 \cdot n \cdot (1 - |n|)$), and ρ_s = –1 for the lower part ($m_v < 2 \cdot n \cdot (1 - |n|)$).

9 Validation of enhanced formula

Fig. 15 shows a comparison of the actual interaction curves (solid blue lines) with the ones produced by the proposed enhanced formula (dotted red lines) for the same example as Fig. 13.

In addition, Fig. 17 shows the loci of the corner points, which are included as dotted green lines. The loci are produced by the parametric coordinates of the corner points, i.e. $(\pm(1 - n^2), 2 \cdot n \cdot (1 - |n|))$, $-1 \le n \le 1$.

It can be seen that the enhanced formula is symmetric only about the v-axis. In addition to the loading cases of N + M_v and M_u + M_v, equilibrium formulae are employed for the case when the orientation of the neutral axis is parallel to the major axis of the section. Thus, very good approximation is

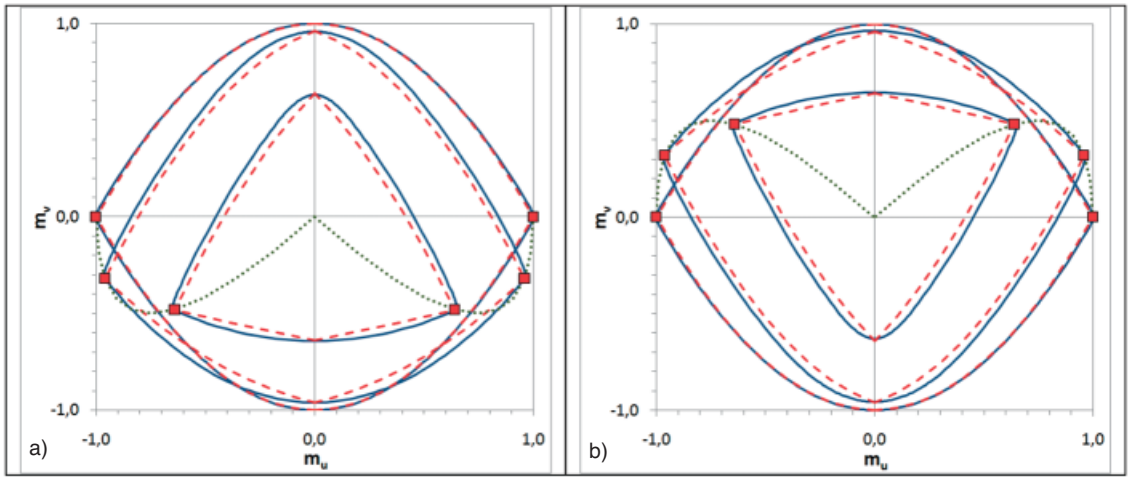

Fig. 15. Interaction curves: exact (blue) and with enhanced formula Eq. (27) (dotted red) for (a) compression (n = 0, –0.2, –0.6) and (b) tension (n = 0, +0.2, +0.6)

also observed at the corner points of the interaction curves, shown as red squares in Fig. 15. For the generic case of N + M_u + M_v, the proposed enhanced formula is practically exact.

10 Examples using the proposed formulae

The legs of a telecommunications tower consist of 160 × 160 × 15 mm angles of grade S 235 material. Their cross-section is to be verified for the following design forces and moments as provided by the structural analysis:

a) N_{Ed} = –800 kN $M_{y,Ed}$ = –4.60 kNm $M_{z,Ed}$ = 2.0 kNm
b) N_{Ed} = –800 kN $M_{y,Ed}$ = 4.60 kNm $M_{z,Ed}$ = 2.0 kNm
c) N_{Ed} = –400 kN $M_{y,Ed}$ = 4.60 kNm $M_{z,Ed}$ = 2.0 kNm

The material safety factor for cross-section verification is γ_{M0} = 1.0.

Cross-section data (Fig. 16):
A = 46.06 cm², I_u = 1747 cm⁴, I_v = 450.8 cm⁴,
u_{max} = 63.5 mm, u_{min} = 49.6 mm

$$v_{max} = \frac{16}{\sqrt{2}} = 11.3\,\text{cm}$$

Cross-section classification:

$$\frac{c}{t} = \frac{h - t - r}{t} = \frac{160 - 15 - 17}{15} = 8.5 < 9$$

→ class 1 (inelastic design is permitted)

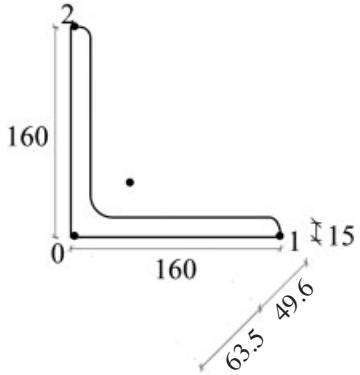

Fig. 16. Cross-section of example showing stress points

$N_{pl,Rd}$ = 46.06 · 23.5 = 1082 kN

$$M_{u,pl,Rd} = 1082 \cdot \frac{16}{2 \cdot \sqrt{2}} = 6121\,\text{kNcm}$$

$$M_{v,pl,Rd} = 1082 \cdot \frac{16}{4 \cdot \sqrt{2}} = 3060\,\text{kNcm}$$

The moments about the principal axes are determined from:

$$M_u = \left(M_y + M_z\right)/\sqrt{2} \quad M_v = \left(M_y - M_z\right)/\sqrt{2}$$

a) $M_{u,Ed}$ = –1.84 kNm $M_{v,Ed}$ = –4.67 kNm

– Elastic design (Fig. 17)

$$N: \sigma_N = -\frac{800}{46.06} = -17.37\,\text{kN/cm}^2 \text{ at all stress points}$$

$$M_u: \sigma_0 = 0\ \sigma_1 = -\sigma_2 = -\frac{-184}{1747} \cdot 11.3 = 1.19\,\text{kN/cm}^2$$

$$M_v: \sigma_o = \frac{-467}{450.8} \cdot 6.35 = -6.58\,\text{kN/cm}^2$$

$$\sigma_1 = \sigma_2 = -\frac{-467}{450.8} \cdot 4.96 = 5.14\,\text{kN/cm}^2$$

Total stresses:

σ_0 = –17.37 – 6.58 = –23.95 kN/cm² > f_y/γ_{M0} = 23.5 kN/cm²
σ_1 = –17.37 + 1.19 + 5.14 = –11.04 kN/cm² < 23.5 kN/cm²
σ_2 = –17.37 – 1.19 + 5.14 = –13.42 kN/cm² < 23.5 kN/cm²

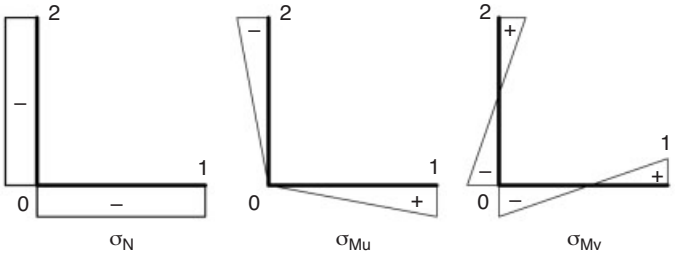

Fig. 17. Stresses of example, case a

Exploitation factor for elastic design: $\nu = \frac{23.95}{23.5} = 1.02$

– Inelastic design with simple formula Eq. (14)

Exploitation factor for inelastic design:

$$\left(\frac{800}{1082} + \frac{184}{6121}\right)^2 + \frac{467}{3060} = 0.74$$

– Inelastic design with enhanced formula Eq. (27)

$$n = \frac{-800}{1082} = -0.739,\ m_u = \frac{-184}{6121} = -0.030,$$
$$m_v = \frac{-467}{3060} = -0.153$$

$$\rho_s = \operatorname{sgn}\left(-0.030 - 2\cdot(-0.739)\cdot\left(1 - \left|-0.739\right|\right)\right)$$
$$= \operatorname{sgn}\left(0.233\right) = 1$$

$$\rho = \left|\frac{(-0.739) - \operatorname{sgn}(-0.739)\sqrt{1 - 2\cdot(-0.739)\cdot\left(1 - \left|-0.739\right|\right)\cdot 1}}{(-0.739)^2 - 1}\right|$$
$$= 0.965$$

Exploitation factor for inelastic design:

(|–0.739| + 0.965 · |–0.030|^2 + 1 · (–0.153) = 0.438

Significant plastic reserve according to the enhanced formula because of the quadrant (see Fig. 18a).

b) $M_{u,Ed}$ = 4.67 kNm $M_{v,Ed}$ = 1.84 kNm

– Elastic design

Using a similar calculation to case a, the total stresses are:

σ_0 = –14.78 kN/cm^2 σ_1 = –22.41 kN/cm^2 σ_2 = –16.37 kN/cm^2

Exploitation factor for elastic design: $\nu = \frac{22.41}{23.5} = 0.95$

– Inelastic design with simple formula Eq. (14)

Exploitation factor for inelastic design:

$$\left(\frac{800}{1082} + \frac{467}{6121}\right)^2 + \frac{184}{3060} = 0.73$$

– Inelastic design with enhanced formula Eq. (27)

$$n = \frac{-800}{1082} = -0.739,\ m_u = \frac{467}{6121} = 0.076,$$
$$m_v = \frac{184}{3060} = 0.060$$

$$\rho_s = \operatorname{sgn}\left(0.060 - 2\cdot(-0.739)\cdot\left(1 - \left|-0.739\right|\right)\right) = \operatorname{sgn}(0.446) = 1$$

$$\rho = \left|\frac{(-0.739) - \operatorname{sgn}(-0.739)\sqrt{1 - 2\cdot(-0.739)\cdot\left(1 - \left|-0.739\right|\right)\cdot 1}}{(-0.739)^2 - 1}\right|$$
$$= 0.965$$

Exploitation factor for inelastic design:

(|–0.739| + 0.965 · |0.076|^2 + 1 · (0.060) = 0.720

Practically the same result because of the quadrant (see Fig. 18b).

c) $M_{u,Ed}$ = 4.67 kNm $M_{v,Ed}$ = 1.84 kNm

– Elastic design

σ_0 = –6.1 kN/cm^2 σ_1 = –13.73 kN/cm^2 σ_2 = –7.69 kN/cm^2

Exploitation factor for elastic design: $\nu = \frac{13.73}{23.5} = 0.58$

– Inelastic design with simple formula Eq. (14)

Exploitation factor for inelastic design:

$$\left(\frac{400}{1082} + \frac{467}{6121}\right)^2 + \frac{184}{3060} = 0.26$$

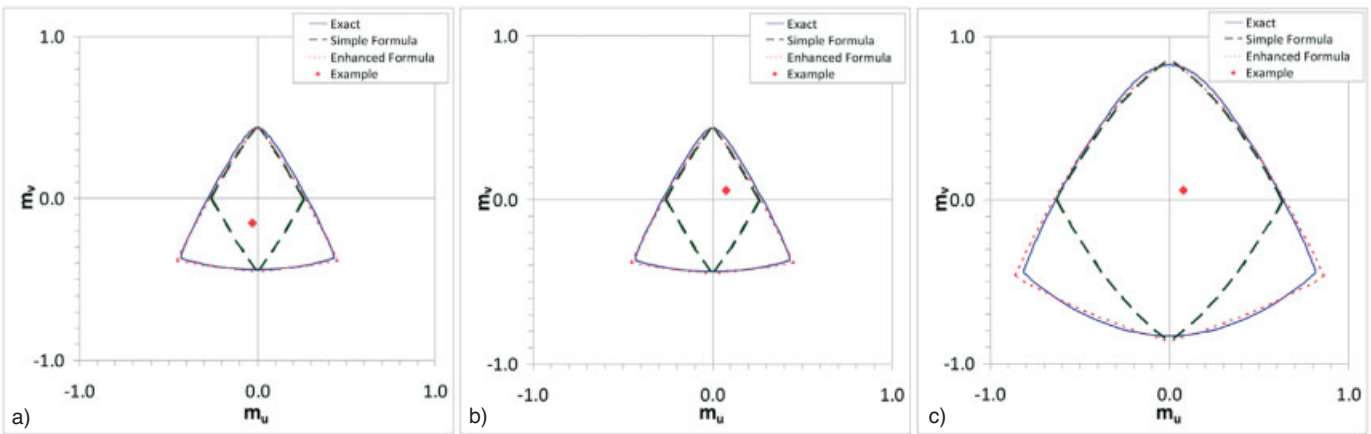

Fig. 18. Interaction curves for examples (a) to (c)

– Inelastic design with enhanced formula Eq. (27)

$$n = \frac{-400}{1082} = -0.370,\ m_u = \frac{467}{6121} = 0.076,$$
$$m_v = \frac{184}{3060} = 0.060$$

$$\rho_s = \operatorname{sgn}\left(0.060 - 2 \cdot (-0.370) \cdot \left(1 - \left|-0.370\right|\right)\right) = \operatorname{sgn}(0.526) = 1$$

$$\rho = \left| \frac{(-0.370) - \operatorname{sgn}(-0.370)\sqrt{1 - 2 \cdot (-0.370) \cdot \left(1 - \left|-0.370\right|\right) \cdot 1}}{(-0.370)^2 - 1} \right| = 0.974$$

Exploitation factor for inelastic design:

$$(|-0.370| + 0.974 \cdot |0.076|^2 + 1 \cdot (0.060) = 0.257$$

Practically the same result because of the quadrant (see Fig. 18c).

The interaction diagrams for the examples are shown in Fig. 18.

11 Conclusions

Appropriate inelastic interaction formulae, Eqs. (14) and (27), for simultaneous biaxial bending around the principal axes and normal force were derived for equal leg angle sections. They allow for a plastic cross-section verification, suitable for angle sections of classes 1 and 2. Eq. (14) is simple but may not fully exhaust the inelastic section reserves for certain sign combinations of axial force and weak axis moment. Eq. (27) almost fully exhausts the section capacity but is a little more complicated.

The numerical results presented indicate that the application of inelastic design may lead to more economical but nevertheless safe designs in practice, as in the case of telecommunications towers. However, this more delicate design should be accompanied by a more elaborate stability analysis.

References

[1] EN 1993-1-1, 2004 Eurocode 3 – Design of steel structures, Part 1-1: General rules and rules for buildings.
[2] *Vayas, I.*: Interaktion der plastischen Grenzschnittgrößen doppelsymmetrischer I-Querschnitte. Stahlbau 69 (2000), H. 9, pp. 693–706.
[3] *Vayas, I.*: Interaktion der plastischen Grenzschnittgrößen doppelsymmetrischer Kastenquerschnitte. Stahlbau 70 (2001), pp. 869–884.
[4] *Scheer, J., Bahr, G.*: Interaktionsdiagramme für die Querschnittstraglasten außermittig längsbelasteter, dünnwandiger Winkelprofile. Bauingenieur 56 (1981), pp. 459–466.
[5] *Charalampakis, A. E., Koumousis, V. K.*: Ultimate strength analysis of composite sections under biaxial bending and axial load. Advances in Engineering Software 39 (2008), pp. 923–936.

Keywords: plastic design; elastic design; angle sections; interaction diagrams; compound biaxial bending

Authors:
Prof. Dr.-Ing. Dr. h.c. Ioannis Vayas, National Technical University of Athens, Laboratory of Steel Structures
Aristotelis Charalampakis, PhD candidate, National Technical University of Athens, Institute of Structural Analysis & Aseismic Research
Prof . Vlasis Koumousis, PhD, National Technical University of Athens, Institute of Structural Analysis & Aseismic Research.